



Lateral Free Vibration Analysis of Axially Functionally Graded Tapered Timoshenko Pipes with Variable Cross-section Supported by Variable Pasternak Foundation

*¹Gbadeyan, J.A., & ²Adeniran, P.O.

¹Department of Mathematics, University of Ilorin, 1515, Ilorin, 240003, Kwara State, Nigeria

²Department of Mathematics, Covenant University, 1023, Ota, 112233, Ogun State, Nigeria.

*Corresponding author email: paul.adeniran@covenantuniversity.edu.ng

Abstract

In this work, the Variational Iteration Method (VIM) is employed to examine the dynamic response of an axially inhomogeneous fluid-conveying pipe resting on a Pasternak elastic foundation. The pipe is modeled using Timoshenko beam theory, which accounts for shear deformation and rotary inertia, and is assumed to have a non-uniform cross-sectional configuration. Along the axial direction, the elastic foundation parameters, as well as the pipe's mechanical and geometric properties including cross-sectional area, second moment of area, material density, and Young's modulus are assumed to vary continuously. Three boundary conditions are considered in the analysis: Pinned–Pinned, Clamped–Pinned, and Clamped–Clamped. The governing coupled partial differential equations are solved using the variational iteration method, and the resulting natural frequencies of the system are evaluated and presented in tabular form. To validate the accuracy and reliability of the proposed approach, the numerical results obtained are compared with those in the literature, demonstrating excellent agreement. A comprehensive parametric study is further conducted to investigate the influence of the material gradient index, pipe non-uniformity parameter, foundation stiffness coefficients, rotary inertia, flow velocity, and mass ratio on the vibrational behavior of the system. The results reveal that, for both clamped–clamped and clamped–pinned boundary conditions and for a fixed value of the non-uniformity parameter, an increase in the material gradient index leads to a decrease in the fundamental (first-mode) natural frequency, while the higher-order natural frequencies increase.

Keywords: Axially Functionally Graded (AFG), Pasternak Foundation, Non-uniform pipe, Timoshenko Pipe Theory, Lateral Vibration

Introduction

Bulk fluids like water, sewage, oil, and natural gas are widely transported between stations via pipelines carrying flowing fluid. The dynamic behavior of these systems has been the focus of numerous studies due to their vital applications in marine engineering, biomedical engineering, aviation, hydropower, nuclear power plants, petroleum transport, and municipal water supply. Vibration in pipelines containing flowing fluid can induce dynamic stresses and significant deformations, which may cause fatigue damage, structural failure, or catastrophic occurrences such as explosions, posing serious safety risks. Consequently, controlling the vibration of piping structures is essential to ensure their safety, reliability, and longevity, making it a significant area of interest for both Researchers and Engineers (Dangal & Ghimire 2019). Furthermore, the design of a fluid-conveying pipe involves, among others, the analysis of dynamic behaviour of such a pipe subjected to various end conditions. In other words, since vibration is one of the most important phases and moreover it (vibration) poses restrictions and limitations in its effectiveness, then thorough understanding of vibration characteristics, particularly natural frequencies become essential. It is therefore important to accurately analyze the vibration characteristics of a pipe with flowing fluid such as natural frequency, among others.

It is remarked at this juncture that fluid-conveying pipe can be classified (just like beams) based on four kinds of classical pipe theories, namely, Euler-Bernoulli pipes, Rayleigh pipes, Shear pipes and Timoshenko pipes. The modeling of internally flowing pipes can vary significantly depending on the inclusion or exclusion of shear deformation and rotary inertia effects. The Euler–Bernoulli pipe model represents the simplest case, where both shear deformation and rotary inertia are neglected. If only shear deformation is accounted for, the system is referred to as a Shear pipe model. In contrast, when only rotary inertia is considered, it is known as a Rayleigh pipe model. The most comprehensive formulation is the Timoshenko pipe model, which incorporates both shear deformation and rotary inertia effects, providing greater accuracy for moderately thick vibrating pipes with flowing fluid. Dagli and Ergut (2019) investigated vibration of pipelines flowing fluid under generalized end conditions. In their study, an assumption of ideal fluid was made while generating the equation governing the motion for a prismatic fluid-transporting pipe. Natural frequencies were determined as functions of fluid velocity and stiffness, with further analysis on the role of rotary inertia and mass ratio in the first three modes. It is also remarked that their work was based on Rayleigh pipe model.

Some relevant and recent works on fluid-conveying Euler-Bernoulli pipes are discussed as follows. Yi-min et al. (2010) used the Eliminated Element-Galerkin approach to investigate the eigenfrequencies of fluid-structure interactions in pipelines carrying moving fluids. They examined different boundary conditions and the effects of mass, stiffness, length, and flow velocity on natural frequencies. Their findings indicated that the Coriolis force has minimal impact, and they are applicable to nuclear plants and other industrial applications. Paidoussis et al. (2014) conducted a thorough analysis of dynamics of fluid-carrying pipelines, discretizing the governing equations of motion using the Galerkin method. They employed the eigenfunctions of a free–free Euler–Bernoulli pipe model as trial functions in their methodology. The Euler-Bernoulli pipe theory was utilized to simulate the transverse vibration behavior of piping systems. In order to provide a basis of reference for upcoming research on fluid-structure interaction in piping systems, the authors determined the dimensionless eigenfrequencies of the system under two different sets of non-classical boundary conditions. Sutar et al. (2018) studied the dynamic response of slender pipe with flowing fluid using Muller’s method. The authors varied the dimensionless velocities to determine the vibrational frequencies of the piping system for all the boundary conditions considered. Ding and Ji (2023) examined the vibration control of Euler-Bernoulli pipeline with flowing fluid: a state of the art was reviewed. It was also reported by Sakar and Ganguli (2014) that Euler-Bernoulli pipe theory can obtain a good approximation for long slender pipes since the theory overestimates natural frequency of the system for short thick pipes. However, it is known that the Timoshenko pipe theory gives a more realistic and accurate representation for short thick pipes. It often leads to two coupled differential equations of motion of internally flowing pipes. Based on the advantage of Timoshenko pipe over Euler-Bernoulli pipe, the former can serve as an alternative strategy in Engineering practice. On this note, some investigators have carried out research on dynamic behaviour of pipes containing flowing fluid via Timoshenko pipe model. In particular, the dynamics of fluid conveying Timoshenko pipeline using Finite Element Method was examined by (Chu and Li 1995). Bozyigit et al. (2018) studied the natural vibration of fluid-transporting Timoshenko pipeline. The authors obtained the natural frequencies, modes and critical flow velocity of the system subjected to different sets of vibrating configurations. Also, the natural frequency and critical velocity were obtained analytically and then compared with those obtained using easy mathematical techniques called DTM and ADM. A very good agreement was found in their comparative studies. Dynamic response of pipe conveying fluid via a coupled Timoshenko model using Finite Difference Method (FDM) was studied by (Ding et al. 2019). The work involved nonlinear coefficients of the transverse vibrating system. It is noted that in all the above previous works on Timoshenko pipes, in particular, only uniform pipes were considered.

Geometric characteristics of non-prismatic elastic pipes, such as area of the cross-section and second moment of area change progressively or slightly across the length of the pipe (Soltani & Asgarian 2019). According to Soltani and Asgarian (2019), non-uniform structures made of functionally graded materials (FGMs) are being increasingly used in the energy and aerospace industries because of their unique characteristics, which include superior weight distribution, heat resistance, and mechanical strength. Gaith (2021) investigated the effects of pipe non-uniform properties on dynamic response by examining the dynamics of pipeline with variable cross-section carrying fluid at steady flow rate. By applying Hamilton’s principle, the governing equation of motion was derived to examine the impact of pipe’s non-uniformity parameter on the eigenfrequencies of the piping systems.

Functionally graded materials (FGMs) represent a class of advanced composites engineered so that their mechanical properties transition gradually between surfaces along a designated spatial direction. These materials were first proposed in Japan in 1984 during the development of a space plane (Elthaher et al., 2010). Since then, they have drawn considerable attention from the research community owing to their remarkable thermal resistance, relatively low weight, and toughness (Chen et al. 2020). For readers seeking an in-depth discussion on

FGMs and their uses, a thorough review is available in (Miyamoto et al. 1999). It is also hereby remarked that, in engineering practice, there exists a number of manufacturing procedures, such as centrifugal electron phoretic deposition and chemical vapour deposition that can be used in the fabrication of FGMs. The study in Yang et al. (2016) explored the natural vibration of internally flowing curved axially functionally graded (AFG) pipes. They used a numerical approach based on the modified inextensible theory to derive the vibration frequency equation and applied the Coupled Mode Method to compute the eigenfrequencies. These results were validated against those from a Finite Element Method study by (Misra et al., 1999). Their parametric analysis revealed that flow velocity, material density, the gradient index of material distribution, and the pipe's opening angle have significant impacts on the vibration frequencies of the piping system. In another work, Zhao et al. (2021) investigated the dynamic behavior of AFG conical pipelines with flowing fluid, focusing on the effects of volume fraction index, reduction factor, and volume fraction function type on vibration frequencies of internally flowing pipelines. They observed a linear decrease in both critical velocity and natural frequency as the reduction factor increases. It is also noted here that their work deals with internally flowing pipes with variable cross-section whose dynamic behaviour is based on Euler-Bernoulli pipe theory. Aghazadeh (2021) examined dynamical characteristics of AFG pipes containing flowing fluid using a higher order shear deformation theory. Differential Quadrature Scheme was utilized to discretize the system of differential equations of their work in order to generate numerical results for the AFG pipes with flowing fluid. The effect of material gradation, fluid velocity, shear deformation profile on the eigenfrequencies of AFG non-uniform pipes with flowing fluid was presented. Yi-Wen and Gui-Lin (2022) investigated dynamic characteristics of functionally graded hot pipelines with flowing fluid. The authors observed that the material gradient index, fluid velocity and temperature decreased the vibration frequencies of the system. The flexural vibration properties of functionally graded (FG) poroelastic Timoshenko pipes with flowing fluid have been the subject of recent research by Ding et al. (2024). Studies on FG Timoshenko pipes with flowing fluid is noticeably lacking, despite significant advancements in the analysis of FG Timoshenko beams (Chen et al. 2020; Huang et al., 2013; Zhao et al., 2017; Ozdemir 2019).

Relatively few studies have addressed the vibration response of pipes with internal flowing fluid supported by elastic foundations. Notably, the influence of foundation support has not been investigated in the literature discussed earlier. Chellapilla and Simha (2007) emphasized that the stability of internally flowing uniform Euler-Bernoulli pipes is significantly improved when supported by a foundation compared to when no foundation is present. Moreover, considerable research has been conducted on the vibrational analysis of both Euler-Bernoulli and Timoshenko beams supported by foundations (Adair et al., 2018; Calim 2016; Tang et al., 2025). However, investigations on internally flowing pipes with foundation support predominantly focus on Euler-Bernoulli pipe models (Gaith 2020; Gbadeyan & Adeniran 2023). Consequently, studies exploring the vibration response of Timoshenko pipes with flowing fluid supported by foundations remain relatively scarce. An exception is the recent work by Askarian et al. (2024), who analyzed the dynamics of fluid-carrying Timoshenko pipes supported by fractional viscoelastic foundations.

Based on the reviewed literature of the above paragraphs, we are inspired to examine, in this paper, the lateral vibration of internally flowing AFG Timoshenko pipes with variable cross-section supported by variable Pasternak subgrade. This type of problem has not been investigated. Specifically speaking, this study is an appropriate extension of the previous works in (Gbadeyan, Adeniran, Idowu, Dada 2025). Hence, the present research work attempts to address this problem which could provide useful information necessary for designing a fluid-carrying Timoshenko pipeline supported by variable two-parameter elastic subgrade

Formulation of the Problem

The lateral free vibration of internally flowing AFG Timoshenko pipes with variable cross-section resting on variable Shear layer foundation is investigated. The coupled governing partial differential equations are expressed as (Bozygit et al. 2018 and Chen et al. 2020)

$$\frac{\partial}{\partial x^*} \left[E(x^*) I(x^*) \frac{\partial \xi_1(x^*, t)}{\partial x^*} \right] + \kappa G(x^*) A(x^*) \left[\frac{\partial w(x^*, t)}{\partial x^*} - \xi_1(x^*, t) \right] - \rho(x^*) I(x^*) \frac{\partial^2 \xi_1(x^*, t)}{\partial t^2} = 0 \quad (1)$$

$$\begin{aligned} & \frac{\partial}{\partial x^*} \left[\kappa G(x^*) A(x^*) \left(\frac{\partial w(x^*, t)}{\partial x^*} - \xi_1(x^*, t) \right) \right] - [m_f + \rho(x^*) A(x^*)] \frac{\partial^2 w(x^*, t)}{\partial t^2} \\ & - m_f V^2 \frac{\partial^2 w(x^*, t)}{\partial x^{*2}} - 2m_f V \frac{\partial^2 w(x^*, t)}{\partial x^* \partial t} \\ & - k_w(x^*) w(x^*, t) + \frac{\partial}{\partial x^*} \left[k_p(x^*) \frac{\partial w(x^*, t)}{\partial x^*} \right] = 0, \quad (0 \leq x^* \leq L) \end{aligned} \quad (2)$$

Here, the transverse displacement and cross-sectional rotation of the pipe at position x^* and time t denoted by $w(x^*, t)$, and $\xi_1(x^*, t)$, respectively. Here, κ is the shear correction factor. The elastic subgrade supporting the

pipes characterized by position-dependent Winkler modulus $k_w(x^*)$ and shear layer of the foundation $k_p(x^*)$. Along the pipe length, the flexural rigidity $E(x^*)I(x^*)$, shear stiffness $G(x^*)A(x^*)$, mass per unit length $\rho(x^*)A(x^*)$, and rotatory inertia $\rho(x^*)I(x^*)$ vary continuously with x^* . The total pipe length is L . The material properties, including elastic modulus $E(x^*)$, shear deformation modulus $G(x^*)$, and material density $\rho(x^*)$, are all functions of the axial position x^* . The fluid flowing in the pipe is described by a constant mass of the fluid m_f and a constant axial flow velocity V .

We assume that the system under consideration is harmonically excited with an angular frequency ω , so that

$$w(x^*, t) = W(x_1)e^{i\omega t} \quad (3)$$

$$\xi_1(x^*, t) = \theta(x_1)e^{i\omega t} \quad (4)$$

where $W(x_1)$, $\theta(x_1)$ and i are the amplitude of the pipe deflection, the amplitude of the pipe bending slope and imaginary unit, respectively.

It follows that in view of equations (3) and (4) above, equations (1) and (2) reduces to the following ordinary differential equations:

$$\frac{d}{dx_1} \left[E(x_1)I(x_1) \frac{d\theta}{dx_1} \right] + \kappa G(x_1)A(x_1) \left[\frac{dW}{dx_1} - \theta \right] + \rho(x_1)I(x_1)\omega^2\theta = 0 \quad (5)$$

$$\begin{aligned} & \frac{d}{dx_1} \left[\kappa G(x_1)A(x_1) \left(\frac{dW}{dx_1} - \theta \right) \right] + [m_f + \rho(x_1)A(x_1)]\omega^2 W \\ & - m_f V^2 \frac{d^2 W}{dx_1^2} - 2m_f V i \omega \frac{dW}{dx_1} \\ & - k_w(x_1)W + \frac{d}{dx_1} \left[k_p(x_1) \frac{dW}{dx_1} \right] = 0 \quad (0 \leq x_1 \leq L) \end{aligned} \quad (6)$$

, respectively

Boundary Conditions

In this present work, unless noted otherwise, three types of vibrating configurations are applied to solve equations (5) and (6): Simply-Supported, Clamped-Clamped, and Clamped-Pinned. Each set of vibrating configurations consists of two end conditions at the pipe's left end $x_1 = 0$ and two at the right end $x_1 = L$: In particular, for Simply-Supported end conditions, we have at $x_1 = 0$;

$$W(0, t) = 0, \quad \frac{d\theta(0,t)}{dx_1} = 0 \quad (7)$$

at $x_1 = L$;

$$W(L, t) = 0, \quad \frac{d\theta(L,t)}{dx_1} = 0 \quad (8)$$

while for Clamped-Clamped end conditions, we have

at $x_1 = 0$;

$$W(0, t) = 0, \quad \theta(0, t) = 0 \quad (9)$$

at $x_1 = L$;

$$W(L, t) = 0, \quad \theta(L, t) = 0 \quad (10)$$

and for Clamped-Pinned pipe

at $x_1 = 0$;

$$W(0, t) = 0, \quad \theta(0, t) = 0 \quad (11)$$

at $x_1 = L$;

$$W(L, t) = 0, \quad \frac{d\theta(L,t)}{dx_1} = 0 \quad (12)$$

In summary, the pertinent boundary-value problems are composed of equations (5) - (12).

2.2 Further simplification of the governing equations of the boundary value problems

Equations (5) - (6) are complex as they include variable coefficients such as $E(x_1)$, $\rho(x_1)$, $A(x_1)$, $I(x_1)$, $k_w(x_1)$ and $k_p(x_1)$. In order to facilitate the analysis, the following dimensionless variables are introduced:

$$\begin{aligned} \bar{W} &= \frac{W}{L}, \quad \bar{x}_1 = \frac{x_1}{L}, \quad P(\bar{x}_1) = \frac{E(x_1)I(x_1)}{E_L I_L}, \quad Q(\bar{x}_1) = \frac{m_f + \rho(x)A(x_1)}{m_f + \rho_L A_L}, \\ R(\bar{x}_1) &= \frac{k_w(x_1)}{k_{wL}}, \quad T(\bar{x}_1) = \frac{k_p(x_1)}{k_{pL}} \\ F(\bar{x}_1) &= \frac{\rho(x_1)I(x_1)}{\rho_L I_L}, \quad N(\bar{x}_1) = \frac{G(x_1)A(x_1)}{G_L A_L} \end{aligned} \quad (13)$$

where $A_L, \rho_L, I_L, G_L, k_{wL}$ and k_{pL} are the values of $A(x_1), \rho(x_1), I(x_1), G(x_1), k_w(x_1)$ and $k_p(x_1)$ at $(x_1 = 0)$ respectively. Hence, the equations governing the motion of an AFG Timoshenko fluid-carrying pipe with variable cross-section supported by a variable Pasternak subgrade

$$\frac{d^2\theta}{d\bar{x}_1^2} + \frac{P'(\bar{x}_1)}{P(\bar{x}_1)} \frac{d\theta}{d\bar{x}_1} + \frac{F(\bar{x}_1)}{P(\bar{x}_1)} r^2 (1 - \beta) \bar{\omega}^2 \theta + \frac{1}{\eta^2} \frac{N(\bar{x}_1)}{P(\bar{x}_1)} \left(\frac{d\bar{W}}{d\bar{x}_1} - \theta \right) = 0 \quad (14)$$

$$\begin{aligned} & \frac{d^2\bar{W}}{d\bar{x}_1^2} + \frac{N'(\bar{x}_1)}{N(\bar{x}_1)} \frac{d\bar{W}}{d\bar{x}_1} - \frac{d\theta}{d\bar{x}_1} - \frac{N'(\bar{x}_1)}{N(\bar{x}_1)} \theta + \frac{Q(\bar{x}_1)}{N(\bar{x}_1)} \bar{\omega}^2 \eta^2 \bar{W} \\ & - \eta^2 \bar{v}^2 \frac{d^2\bar{W}}{d\bar{x}_1^2} - 2i\bar{v}\beta^{\frac{1}{2}} \bar{\omega} \eta^2 \sqrt{\frac{1}{N(\bar{x}_1)}} \frac{d\bar{W}}{d\bar{x}_1} \\ & - \eta^2 \bar{K}_w \frac{R(\bar{x}_1)}{N(\bar{x}_1)} \bar{W} + \eta^2 G_p \frac{T(\bar{x}_1)}{N(\bar{x}_1)} \frac{d^2\bar{W}}{d\bar{x}_1^2} + \eta^2 G_p \frac{T'(\bar{x}_1)}{N(\bar{x}_1)} \frac{d\bar{W}}{d\bar{x}_1} = 0 \end{aligned} \quad (15)$$

where

$$\begin{aligned} \bar{K}_w &= \frac{k_{wL} L^4}{E_L I_L}, & G_p &= \frac{k_{pL} L^2}{E_L I_L}, & \bar{v} &= \left(\frac{m_f}{N(\bar{x}) E_L I_L} \right)^{\frac{1}{2}} V L, & r^2 &= \frac{I_L}{A_L L^2} \\ \eta^2 &= \frac{E_L I_L}{\kappa G_L A_L L^2}, & \bar{\omega} &= \omega \sqrt{\frac{(m_f + \rho_L A_L) L^4}{E_L I_L}}, & \beta &= \frac{m_f}{m_f + \rho_L A_L} \end{aligned}$$

Here, $K_w, G_p, r, \bar{v}, \eta, \bar{\omega}$ and β are the dimensionless Winkler foundation constant, shear foundation parameter, dimensionless rotatory inertia parameter, dimensionless fluid velocity, dimensionless shear deformation parameter, dimensionless frequency parameter and dimensionless mass ratio, respectively.

For simplicity, the following variable coefficients are also defined:

$$\begin{aligned} \bar{Y}_1(\bar{x}_1) &= \frac{P'(\bar{x}_1)}{P(\bar{x}_1)}, & \bar{Y}_2(\bar{x}_1) &= \frac{F(\bar{x}_1)}{P(\bar{x}_1)}, & \bar{Y}_3(\bar{x}_1) &= \frac{N(\bar{x}_1)}{P(\bar{x}_1)} \\ \bar{Y}_4(\bar{x}_1) &= \frac{N'(\bar{x}_1)}{N(\bar{x}_1)}, & \bar{Y}_5(\bar{x}_1) &= \frac{Q(\bar{x}_1)}{N(\bar{x}_1)}, & \bar{Y}_6(\bar{x}_1) &= \sqrt{\frac{1}{N(\bar{x}_1)}} \\ \bar{Y}_7(\bar{x}_1) &= \frac{R(\bar{x}_1)}{N(\bar{x}_1)}, & \bar{Y}_8(\bar{x}_1) &= \frac{T(\bar{x}_1)}{N(\bar{x}_1)}, & \bar{Y}_9(\bar{x}_1) &= \frac{T'(\bar{x}_1)}{N(\bar{x}_1)} \end{aligned}$$

It is hereby remarked at this juncture, therefore, that the dimensionless governing equations of motion can then be written as

$$\frac{d^2\theta}{d\bar{x}_1^2} + \bar{Y}_1(\bar{x}_1) \frac{d\theta}{d\bar{x}_1} + \bar{Y}_2(\bar{x}_1) r^2 (1 - \beta) \bar{\omega}^2 \theta + \frac{1}{\eta^2} \bar{Y}_3(\bar{x}_1) \left(\frac{d\bar{W}}{d\bar{x}_1} - \theta \right) = 0 \quad (16)$$

$$\begin{aligned} & \frac{d^2\bar{W}}{d\bar{x}_1^2} + \bar{Y}_4(\bar{x}_1) \frac{d\bar{W}}{d\bar{x}_1} - \frac{d\theta}{d\bar{x}_1} - \bar{Y}_4(\bar{x}_1) \theta + \bar{Y}_5(\bar{x}_1) \bar{\omega}^2 \eta^2 \bar{W} \\ & - \eta^2 \bar{v}^2 \frac{d^2\bar{W}}{d\bar{x}_1^2} - 2i\bar{v}\beta^{\frac{1}{2}} \bar{\omega} \eta^2 \bar{Y}_6(\bar{x}_1) \frac{d\bar{W}}{d\bar{x}_1} \\ & - \eta^2 \bar{K}_w \bar{Y}_7(\bar{x}_1) \bar{W} + \eta^2 G_p \bar{Y}_8(\bar{x}_1) \frac{d^2\bar{W}}{d\bar{x}_1^2} + \eta^2 G_p \bar{Y}_9(\bar{x}_1) \frac{d\bar{W}}{d\bar{x}_1} = 0 \end{aligned} \quad (17)$$

In view of equation (13), the end conditions in subsection (2.1) becomes for a Simply-Supported pipe, at $\bar{x}_1 = 0$;

$$\bar{W}(0) = 0, \quad \frac{d\theta(0)}{d\bar{x}_1} = 0 \quad (18)$$

at $\bar{x}_1 = 1$;

$$\bar{W}(1) = 0, \quad \frac{d\theta(1)}{d\bar{x}_1} = 0 \quad (19)$$

, while

for a Clamped-Clamped pipe, we have

at $\bar{x}_1 = 0$;

$$\bar{W}(0, t) = 0, \quad \theta(0) = 0 \quad (20)$$

at $\bar{x}_1 = 1$;

$$\bar{W}(1) = 0, \quad \theta(1) = 0 \quad (21)$$

, and

for a Clamped-Pinned pipe

at $\bar{x}_1 = 0$;

$$\bar{W}(0) = 0, \quad \theta(0) = 0 \quad (22)$$

at $\bar{x}_1 = 1$;

$$\overline{W}(1) = 0, \quad \frac{d\theta(1)}{d\overline{x}_1} = 0 \quad (23)$$

It is remarked, at this juncture, that the above analysis holds for either variable or constant velocity of the fluid in the pipe. Finally, the three non-dimensional boundary value problems to be solved in the present study are now reduced to solving the coupled simultaneous differential equations (16) and (17) subjected to each of the equations ((18), (19)), ((20), (21)) and ((22), (23)), respectively.

Variational Iteration Method (VIM) and its Application

Due to the complexity and variable coefficients in the coupled governing equations of motion, obtaining an exact analytical solution is impractical. Therefore, the Variational Iteration Method (VIM), as introduced by Chen et al. (2020), is utilized as a semi-analytical technique to compute the natural frequencies of free vibration for an AFG fluid-carrying pipe with variable cross-section supported by a variable Shear layer foundation. The analysis is based on Timoshenko pipe theory. To illustrate the application of VIM, we consider a general nonlinear differential equation of the form

$$Q_1[\overline{W}(\overline{x}_1)] + N_1[\overline{W}(\overline{x}_1)] = g_1(\overline{x}_1) \quad (24)$$

Here, N_1 is the non-linear operator, Q_1 is the linear operator of the highest derivative and $g_1(\overline{x}_1)$ is the continuous function. Solving equation (24) via VIM technique, a correction functional of the form

$$\overline{W}_{m+1}(\overline{x}_1) = \overline{W}_m(\overline{x}_1) + \int_0^{\overline{x}_1} \lambda(\zeta) [Q_1 \overline{W}_m(\zeta) + N \overline{W}_m^*(\zeta) - g(\zeta)] d\zeta \quad (25)$$

must be constructed. Here, in equation (25), $\lambda(\zeta)$ is a general Lagrange multiplier whose exact expression can be optimally obtained via variational theory, \overline{W}_m^* is a restricted term which is such that $\delta \overline{W}_m^* = 0$ and \overline{W}_m is the m th approximation. In view of equation (25), the correction functional for the dimensionless governing equations (16) and (17) can be written as:

$$\begin{aligned} \theta_{m+1}(\overline{x}_1) &= \theta_m(\overline{x}_1) + \int_0^{\overline{x}_1} \lambda_1(\zeta) [\theta_{m''}(\zeta) + \overline{Y}_1(\zeta)\theta_{m'}(\zeta) \\ &+ \overline{Y}_2(\zeta)r^2(1-\beta)\overline{\omega}^2\theta_m(\zeta) + \frac{1}{\eta^2}\overline{Y}_3(\zeta)(\overline{W}_{m'}(\zeta) - \theta_m(\zeta))] d\zeta \end{aligned} \quad (26)$$

$$\begin{aligned} \overline{W}_{m+1}(\overline{x}_1) &= \overline{W}_m(\overline{x}_1) + \int_0^{\overline{x}_1} \lambda_2(\zeta) [\overline{W}_{m''}(\zeta) + \overline{Y}_4(\tau)\overline{W}_{m'}(\zeta) - \theta_{m'}(\tau) \\ &- \overline{Y}_4(\tau)\theta_m(\tau) + \overline{Y}_5(\zeta)\overline{\omega}^2\eta^2\overline{W}_m(\zeta) - \eta^2\overline{v}^2\overline{W}_{m''}(\zeta) \\ &- 2\overline{Y}_6(\zeta)i\overline{v}\beta^{\frac{1}{2}}\overline{\omega}\eta^2\overline{W}_{m'}(\zeta) - \overline{Y}_7(\zeta)\eta^2\overline{K}_w\overline{W}_m(\zeta) \\ &+ \overline{Y}_8(\zeta)\eta^2G_p\overline{W}_{m''}(\zeta) + \overline{Y}_9(\zeta)\eta^2G_p\overline{W}_{m'}(\zeta)] d\zeta \end{aligned} \quad (27)$$

, respectively.

Taking the variation of both sides of equations (26) and (27), we have

$$\begin{aligned} \delta\theta_{m+1}(\overline{x}_1) &= \delta\theta_m(\overline{x}_1) + \int_0^{\overline{x}_1} \lambda_1(\zeta) \delta[\theta_{m''}(\zeta) + \overline{Y}_1(\zeta)\theta_{m'}(\zeta) \\ &+ \overline{Y}_2(\zeta)r^2(1-\beta)\overline{\omega}^2\theta_m(\zeta) + \frac{1}{\eta^2}\overline{Y}_3(\zeta)(\overline{W}_{m'}(\zeta) - \theta_m(\tau))] d\zeta \end{aligned} \quad (28)$$

$$\begin{aligned} \delta\overline{W}_{m+1}(\overline{x}_1) &= \delta\overline{W}_m(\overline{x}_1) + \int_0^{\overline{x}_1} \lambda_2(\zeta) \delta[\overline{W}_{m''}(\zeta) + \overline{Y}_4(\zeta)\overline{W}_{m'}(\zeta) - \theta_{m'}(\zeta) \\ &- \overline{Y}_4(\zeta)\theta_m(\zeta) + \overline{Y}_5(\zeta)\overline{\omega}^2\eta^2\overline{W}_m(\zeta) - \eta^2\overline{v}^2\overline{W}_{m''}(\zeta) \\ &- 2\overline{Y}_6(\zeta)i\overline{v}\beta^{\frac{1}{2}}\overline{\omega}\eta^2\overline{W}_{m'}(\zeta) - \overline{Y}_7(\tau)\eta^2\overline{K}_w\overline{W}_m(\zeta) \\ &+ \overline{Y}_8(\zeta)\eta^2G_p\overline{W}_{m''}(\zeta) + \overline{Y}_9(\zeta)\eta^2G_p\overline{W}_{m'}(\zeta)] d\zeta \end{aligned} \quad (29)$$

Determination of the Lagrange multiplier $\lambda(\zeta)$ requires imposing the stationary condition by setting the differential coefficients of equations (28) and (29) to zero. By applying integration by parts and nullifying the variation's coefficients, we obtain:

$$\delta\theta_m: \quad 1 - \lambda_1 + \lambda_1\overline{Y}_1|_{\zeta=\overline{x}_1} = 0 \quad (30)$$

$$\delta\overline{W}'_m: \quad \frac{1}{\eta^2}\overline{Y}_3\lambda_1|_{\zeta=\overline{x}_1} = 0 \quad (31)$$

$$\delta\theta'_m: \quad \lambda_1|_{\zeta=\overline{x}_1} = 0 \quad (32)$$

, and

$$\begin{aligned}
 \overline{W}_1(\overline{x}_1) &= \overline{W}_0(\overline{x}_1) + \int_0^{\overline{x}_1} (\zeta - \overline{x}_1)[\overline{W}''_0(\zeta) + \overline{Y}_4(\zeta)\overline{W}'_0(\zeta) - \theta'_0(\zeta) \\
 &\quad - \overline{Y}_4(\zeta)\theta_0(\zeta) + \overline{Y}_5(\zeta)\overline{\omega}^2\eta^2\overline{W}_0(\zeta) - \eta^2\overline{v}^2\overline{W}''_0(\zeta) \\
 &\quad - 2\overline{Y}_6(\zeta)i\overline{v}\beta^{\frac{1}{2}}\overline{\omega}\eta^2\overline{W}'_0(\zeta) - \overline{Y}_7(\zeta)\eta^2\overline{K}_w\overline{W}_0(\zeta) \\
 &\quad + \overline{Y}_8(\zeta)\eta^2G_p\overline{W}''_0(\zeta) + \overline{Y}_9(\zeta)\eta^2G_p\overline{W}'_0(\zeta)]d\zeta \\
 &\quad \text{.....} \\
 \overline{W}_k(\overline{x}_1) &= \overline{W}_{k-1}(\overline{x}_1) + \int_0^{\overline{x}_1} (\zeta - \overline{x}_1)[\overline{W}''_{k-1}(\zeta) + \overline{Y}_4(\zeta)\overline{W}'_{k-1}(\zeta) - \theta'_{k-1}(\zeta) \\
 &\quad - \overline{Y}_4(\zeta)\theta_{k-1}(\zeta) + \overline{Y}_5(\zeta)\overline{\omega}^2\eta^2\overline{W}_{k-1}(\zeta) - \eta^2\overline{v}^2\overline{W}''_{k-1}(\zeta) \\
 &\quad - 2\overline{Y}_6(\zeta)i\overline{v}\beta^{\frac{1}{2}}\overline{\omega}\eta^2\overline{W}'_{k-1}(\zeta) - \overline{Y}_7(\zeta)\eta^2\overline{K}_w\overline{W}_{k-1}(\zeta) \\
 &\quad + \overline{Y}_8(\zeta)\eta^2G_p\overline{W}''_{k-1}(\zeta) + \overline{Y}_9(\zeta)\eta^2G_p\overline{W}'_{k-1}(\zeta)]d\zeta
 \end{aligned} \tag{48}$$

The solution of equations (16) and (17) can be expressed as

$$\theta(\overline{x}_1) = \lim_{k \rightarrow \infty} \theta_k(\overline{x}_1) \tag{49}$$

$$\overline{W}(\overline{x}_1) = \lim_{k \rightarrow \infty} \overline{W}_k(\overline{x}_1) \tag{50}$$

Here, and for numerical purpose, a large value of k equals to m is chosen instead of infinity and then substituted into equations (47) and (48) to obtain an approximate solution

$$\theta(\overline{x}_1) = \theta_m(\overline{x}_1) \tag{51}$$

$$\overline{W}(\overline{x}_1) = \overline{W}_m(\overline{x}_1) \tag{52}$$

To simplify the analysis, equations (51 and 52) are incorporated into the boundary conditions, resulting in a set of four simultaneous equations that may be built into the following matrix representation:

$$\begin{pmatrix} P_{11}^{(k)}(\overline{\omega}_j^j) & P_{12}^{(k)}(\overline{\omega}_j^m) & P_{13}^{(k)}(\overline{\omega}_j^m) & P_{14}^{(k)}(\overline{\omega}_j^m) \\ P_{21}^{(k)}(\overline{\omega}_j^m) & P_{22}^{(k)}(\overline{\omega}_j^m) & P_{23}^{(k)}(\overline{\omega}_j^m) & P_{24}^{(k)}(\overline{\omega}_j^m) \\ P_{31}^{(k)}(\overline{\omega}_j^m) & P_{32}^{(k)}(\overline{\omega}_j^m) & P_{33}^{(k)}(\overline{\omega}_j^m) & P_{34}^{(k)}(\overline{\omega}_j^m) \\ P_{41}^{(k)}(\overline{\omega}_j^m) & P_{42}^{(k)}(\overline{\omega}_j^m) & P_{43}^{(k)}(\overline{\omega}_j^m) & P_{44}^{(k)}(\overline{\omega}_j^m) \end{pmatrix} \begin{pmatrix} a \\ b \\ c \\ d \end{pmatrix} = \begin{pmatrix} 0 \\ 0 \\ 0 \\ 0 \end{pmatrix} \tag{53}$$

In equation (53), the entries of the 4×4 matrix, $S_{pq}^{(k)}(\overline{\omega}_j^m)$, $p = 1 - 4$; $q = 1 - 4$ denotes the evaluated polynomial of the eigenvalues and other parameters of the AFG non-prismatic fluid-carrying pipe lying on a variable Pasternak subgrade. A non-trivial solution to the free vibration eigenvalue problem of AFG pipes is obtained when the determinant of the corresponding coefficient matrix equals zero.

This reduces to a characteristic equation in the form of a polynomial whose roots correspond to eigenvalue $\overline{\omega}_i^m$. Hence, the resulting characteristics polynomial is numerically solved to obtain the natural frequency of the system.

Results

This section presents numerical results illustrating the dynamic response of axially functionally graded (AFG), non-prismatic fluid-conveying pipes supported by a spatially varying Pasternak elastic foundation. The analysis considers three boundary conditions: Clamped–Pinned (C–P), Clamped–Clamped (C–C), and Pinned–Pinned (P–P). In this study, the fluid velocity is assumed to remain constant along the length of the pipe.

The explicit expressions of the material properties, geometric properties, and foundation parameters are adopted from Chen et al. (2020) and are specified below for all numerical cases considered in this work.

It is further assumed that the material properties of the pipe vary along its length according to a power-law distribution of the form:

$$E(\overline{x}_1) = E_L \left(1 + \left(\frac{E_L - E_R}{E_R} \right) \overline{x}_1^n \right), \tag{54}$$

$$\rho(\overline{x}_1) = \rho_L \left(1 + \left(\frac{\rho_L - \rho_R}{\rho_R} \right) \overline{x}_1^n \right), \tag{55}$$

, respectively,

where n is the spatial material gradient index, \bar{x}_1 is the non-dimensional axial coordinate along the pipe length, E_L , E_R , ρ_L and ρ_R are the Young's modulus of the left and right ends of the pipe, mass density at the left and right ends of the pipe, respectively.

Also, the main constituents of the AFG materials of the pipeline with flowing fluid considered in this work are Alumina (Al_2O_3) and Zirconia (ZrO_2), whose properties are: Al_2O_3 : $E_L = 70GPa$, $\rho_L = 2702kg/m^3$ and ZrO_2 : $E_R = 200GPa$, $\rho_R = 5700kg/m^3$, respectively [28].

Next, the Area of cross-section $A(\bar{x}_1)$ and the Second moment of area $I(\bar{x}_1)$ are assumed to vary along the pipe axis as follows:

$$A(\bar{x}_1) = A_L(1 - \alpha\bar{x}_1) \quad (56)$$

$$I(\bar{x}_1) = I_L(1 - \alpha\bar{x}_1)^3 \quad (57)$$

where A_L, I_L are the area of the cross-section and the second moment of area at the left end of the pipe, respectively and α is the non-uniform parameter of the pipe.

The elastic modulus of the Winkler foundation $k_w(\bar{x}_1)$ along with the shear stiffness of the foundation $k_p(\bar{x}_1)$ are assumed to have a linear variation with respect to \bar{x}_1 expressed as follows:

$$k_w(\bar{x}_1) = k_{wL}(1 - \xi\bar{x}_1) \quad (58)$$

$$k_p(\bar{x}_1) = k_{pL}(1 - \xi\bar{x}_1) \quad (59)$$

where ξ is the non-prismatic foundation stiffness, k_{wL} and k_{pL} are the foundation elastic moduli for Winkler and shear parameters at the left end of the pipe, respectively.

The first numerical results aim to assess the validity and accuracy of the proposed method by benchmarking the VIM results against those available in the published literature. Here, some of the data used for all the numerical computations of the natural frequencies of the present work are rotatory inertia $r = 0.1$, shear correction factor $\kappa = \frac{5}{6}$, and the ratio of Young's modulus to shear modulus $\frac{E_L}{G_L} = 2.6$ respectively, except otherwise stated.

Moreover, using the semi-analytical method proposed in this work, the impacts of non-prismatic parameters, material non-homogeneity parameters, mass ratio, flow velocity and foundation stiffness on the vibration characteristics of an internally flowing AFG pipe supported by a Pasternak elastic subgrade are then determined and discussed. The variety of computer programs for the relevant numerical computations using the variational iteration technique are developed with the aid of MAPLE software.

Validation of the present model

For the purpose of validating the present model, four (4) special problems are considered in this subsection. These are (i) the problem of determining the eigenfrequencies of non-AFG prismatic Timoshenko pipes without fluid flow (beam) supported by a foundation (ii) the problem involving the investigation of dynamic response of tapered, non-AFG Timoshenko pipes with no fluid flow and without a foundation (iii) the problem of investigating natural vibration of internally flowing AFG Timoshenko pipes (with no fluid flow) not supported by a foundation and (iv) the problem of dynamic characteristics of uniform non-AFG Timoshenko pipes (having no fluid flow) supported by a Pasternak elastic subgrade. It is remarked at this juncture, that for each of the four special problems mentioned above, a Timoshenko pipe for which there is no fluid flow (a 'beam') is considered and hence the comparison are carried out using the existing results for Timoshenko beam (Soares et al., 2017; Adair et al., 2018). This is as a result of, to the best of our knowledge, the dearth of similar earlier studies which examined the free vibration of AFG Timoshenko non-uniform pipes with flowing fluid variable supported by variable elastic subgrade. The numerical result obtained for the four special problems are presented in Tables 1-5 and discussed below. New numerical results concerning the influence of the flow velocity, gradient index parameter, the mass ratio and Pasternak foundation parameters on the eigenfrequencies of the AFG, fluid-carrying pipes with variable cross-section supported by Pasternak foundation are then obtained and presented both in Tables and Figures in this section.

Special Problem 1: Uniform Homogeneous Timoshenko pipes with no fluid flow and not lying on a foundation

Table 1 presents the first four dimensionless eigenfrequencies of the free vibration of a uniform non-AFG thick pipe with no fluid flow ('beam'). The pipe does not rest on any foundation. The Clamped-Pinned, Simply Supported and Clamped-Clamped boundary conditions are considered in this numerical example. This problem was earlier on studied (as an example) by (Huang et al. 2013, Tang et al. 2014; Zhao et al. 2017) using different approaches. It should be remarked here that the effects of non-uniform parameter, FGMs and Shear elastic layer of the foundation are neglected. Note that the data used in this computation are: $r = 0.1$, $\alpha = 0$, $\frac{E_L}{G_L} = 2.6$, $\beta = 0$, $\xi = 0$, $\bar{v} = 0$, $\bar{K}_w = 0$, and $G_p = 0$ and most of them are gotten from the work of (Huang et al. 2013). In

addition, it can be seen from Table 1 that the results obtained using VIM correspond well with those obtained by Huang et al. (2013) using Green’s Function (GF), Tang et al. (2014) using Analytical Method (ANM) and Zhao et al. (2017) using Chebyshev Polynomial Theory (CPT) for the three vibrating configurations. Note also that $\beta = 0$ implies $m_f = 0$

Table 1: Comparison of the first four dimensionless eigenfrequencies of non-AFG prismatic Timoshenko pipes with no fluid flow and not supported by foundation

End conditions	Methods	$\bar{\omega}_1$	$\bar{\omega}_2$	$\bar{\omega}_3$	$\bar{\omega}_4$
Clamped-Pinned	Present (VIM)	11.0825	27.1144	44.8446	59.2034
	G.F	11.0825	27.1144	44.8446	59.2034
	ANM	11.0825	27.1144	44.8446	59.2034
	CPT	11.0825	27.1144	44.8446	59.2034
Clamped-Clamped	Present (VIM)	13.8348	28.5179	45.6672	61.8677
	G.F	13.8348	28.5179	45.6672	61.8677
	ANM	13.8348	28.5179	45.6672	61.8677
	CPT	13.8348	28.5179	45.6672	61.8677
Pinned-Pinned	Present (VIM)	9.1607	31.0643	58.1930	86.9867
	G.F	9.1607	31.0643	58.1930	86.9867
	ANM	9.1607	31.0643	58.1930	86.9867
	CPT	9.1607	31.0643	58.1930	86.9867

Special Problem 2: Non-uniform Homogeneous Timoshenko pipes not lying on a foundation

The lowest four dimensionless eigenfrequencies of a non-AFG non-prismatic Timoshenko pipe subjected to each of the Clamped-Clamped and Simply-Supported end conditions are presented in Tables 2 and 3, respectively. It is assumed that the pipe does not rest on a foundation. Here, an expression for a case of linearly varying depth and constant height was considered (see equation 56). This special problem neglects the impact of material gradient index parameters, fluid flow velocity, mass ratio and foundation stiffnesses on the eigenfrequencies of the pipeline systems. In Table 2, the values used for the non-uniform parameter α are 0.2, 0.4, 0.6 and 0.8 under Clamped-Clamped vibrating configuration. It can be seen that the numerical results obtained using VIM show excellent agreement with those gotten by Huang et al. (2013) who utilize Green’s function (GF). Also, Table 3 gives the numerical results of vibrational frequencies with various values of α for Pinned-Pinned end conditions while $n = \beta = \xi = \bar{v} = \bar{K}_w = G_p = 0$. It can be observed from Table 3 that eigenfrequencies obtained by VIM excellently agree with the results obtained by Shahba et al. (2010) who used Differential Transformation Method (DTM) and Auciello and Ercolano (2004) employing Rayleigh-Ritz Method (RRM) to solve the same problem. Tables can be inserted via the normal table and tabular environment.

Table 2: The first four non-dimensional eigenfrequencies of a non-prismatic non-AFG Clamped-Clamped Timoshenko pipe (with no fluid flow) not resting on a foundation

α	Methods	$\bar{\omega}_1$	$\bar{\omega}_2$	$\bar{\omega}_3$	$\bar{\omega}_4$
0.2	Present (VIM)	13.2223	27.7782	44.6971	61.8066
	G.F	13.2223	27.7782	44.6971	61.8066
0.4	Present (VIM)	12.4222	26.7234	43.3623	60.7136
	G.F	12.4222	26.7234	43.3623	60.7136
0.6	Present (VIM)	11.3341	25.1246	41.3345	58.6324
	G.F	11.3341	25.1246	41.3345	58.6324
0.8	Present (VIM)	9.7271	22.4303	37.7417	54.4994
	G.F	9.7271	22.4303	37.7417	54.4994

Table 3: Vibration of a non-prismatic non-AFG Timoshenko Pinned-Pinned Timoshenko pipe (with no fluid flow) not resting on a foundation Note: RRM denotes Rayleigh-Ritz Method

α	Methods	$\bar{\omega}_1$	$\bar{\omega}_2$	$\bar{\omega}_3$	$\bar{\omega}_4$
0.5	DTM	6.754	24.353	47.281	72.629
	RRM	6.765	24.462	47.371	72.674
	Present(VIM)	6.754	24.353	47.281	72.629
0	DTM	9.022	29.901	55.173	81.754
	RRM	9.023	29.914	55.201	81.817
	Present (VIM)	9.022	29.901	55.173	81.754
-1	DTM	11.893	36.403	62.798	67.976
	RRM	11.901	36.427	63.004	68.143
	Present (VIM)	11.893	36.403	62.794	67.976

Special Problem 3: Non-uniform Timoshenko pipes with AFG material but not resting on a foundation

Table 4 shows a comparison between the results obtained from the present work and the results gotten from Chen et al. (2020) who used Variational Iteration Method (VIM) and Huang et al. (2013) who used Green’s Function (GF) for the dimensionless frequencies of AFG variable cross-sectional Timoshenko pipes (with no fluid flow) and without a foundation. The numerical example was subjected to Clamped-Clamped and Clamped-Pinned end conditions respectively with various values of non-homogeneous gradient index. The data used in this analysis are $\alpha = 0.1$, $\beta = 0$, $\bar{v} = 0$, $\xi = 0$, $\bar{K}_w = 0$ and $G_p = 0$. As shown in Table 4, the eigenfrequencies align closely with previously published results, confirming the validity of the present approach.

Table 4: Variation of a non-prismatic AFG Timoshenko pipe (with no fluid flow) not resting on a foundation

Boundary condition	n	Methods	$\bar{\omega}_1$	$\bar{\omega}_2$	$\bar{\omega}_3$	$\bar{\omega}_4$
Clamped-Clamped	1	Present (VIM)	12.682	26.494	42.647	58.661
		Chen et al (2020)	12.682	26.491	42.642	58.652
		Huang et al (2013)	12.682	26.491	42.642	58.668
	2	Present (VIM)	12.463	26.380	42.964	59.394
		Chen et al (2020)	12.463	26.380	42.961	59.392
		Huang et al (2013)	12.463	26.380	42.961	59.402
	3	Present (VIM)	12.375	26.319	43.083	59.948
		Chen et al (2020)	12.375	26.319	43.083	59.689
		Huang et al (2013)	12.375	26.319	43.084	59.699
	4	Present (VIM)	12.362	26.312	43.135	59.806
		Chen et al (2020)	12.362	26.312	43.135	59.806
		Huang et al (2013)	12.362	26.312	43.135	59.815
Clamped-Pinned	1	Present (VIM)	10.885	25.566	42.183	58.134
		Chen et al (2020)	10.885	25.566	42.183	58.134
		Huang et al (2013)	10.885	25.566	42.183	58.143
	2	Present (VIM)	10.801	25.619	42.650	58.854
		Chen et al (2020)	10.801	25.618	42.647	58.853
		Huang et al (2013)	10.801	25.618	42.648	58.859
	3	Present (VIM)	10.736	25.635	42.855	59.087
		Chen et al (2020)	10.739	25.635	42.855	59.087
		Huang et al(2013)	10.739	26.635	42.855	59.094
	4	Present (VIM)	10.716	25.667	43.956	59.142
		Chen et al (2020)	10.716	25.667	42.956	59.142
		Huang et al (2013)	10.716	25.667	42.956	59.147

Special Problem 4: Uniform non-AFG Timoshenko pipes on non-variable Pasternak subgrade

In Table 5, the first four dimensionless eigenfrequencies for a uniform non-AFG Timoshenko pipe subject to no fluid flow supported by a Pasternak elastic subgrade with constant coefficients are presented. The present results obtained are benchmarked against those by Adair et al. (2018) (using VIM) and Soares et al. (2017) (using Finite Element Method). The Pinned–Pinned configuration is used, along with the material properties: length of the pipe $L = 0.5m$, modulus of elasticity $E_L = 210GPa$, shear modulus $G_L = 80.8GPa$, shear correction factor $\kappa = \frac{5}{6}$ and mass density $\rho_L = 7850kg/m^3$. Also, the following data $\bar{v} = 0$, $\beta = 0$, $\alpha = 0$, $n = 0$, and $\xi = 0$ are used. A good agreement between the current and previously published results supports the reliability of the present

methodology. This agreement, alongside the consistent findings in Tables 1 - 5, affirms the effectiveness and accuracy of the VIM applied.

Table 5: Vibration of a non-AFG uniform Pinned-Pinned Timoshenko pipe (with no fluid flow) supported by a prismatic Shear layer foundation

$K_w = K_p$	r	modes	Present (VIM)	Adair et al (2018)	Soares et al. (2017)
0	0.04	1	3958.50	3959.01	3958.50
		2	14609.40	14610.32	14609.40
		3	29573.30	29574.22	29573.35
		4	46937.00		46937.03
0	0.08	1	7304.70		7304.70
		2	23468.50		23468.52
		3	42396.20		42396.21
		4	61975.50		61975.55
2.5	0.04	1	5209.23	5209.46	5209.24
		2	15965.20	15965.47	15965.20
		3	31051.70	31051.88	31051.70
		4	48571.70		48571.37
2.5	0.08	1	9893.10		9893.10
		2	26642.00		26642.00
		3	46360.40		46360.43
		4	87512.80		87512.80

Effect of non-uniform term α and material non-homogeneity parameter n on eigenfrequencies of an AFG fluid flowing Timoshenko pipe supported by a bi-parametric elastic subgrade

For the purpose of examining the impact of both α and n on the vibration characteristics of AFG Timoshenko pipe with variable cross-section supported by a variable Pasternak subgrade, the first four dimensionless eigenfrequencies of the system under consideration are computed and presented in Tables 6-8 for various values of α and n . Three vibrating configurations namely: Pinned-Pinned (PP), Clamped-Pinned (CP) and Clamped-Clamped (CC) vibrating configurations are also considered for $\xi = 0.2, \beta = 0.1, \bar{v} = 1, G_p = 1, \bar{K}_w = 100$. From Tables 6-8, it can be observed that (a) for Pinned-Pinned vibrating configuration (see Table 6) and for a fixed value of n , the fundamental frequency ($\bar{\omega}_1$) increases, while each of the non-fundamental frequencies ($\bar{\omega}_2, \bar{\omega}_3, \bar{\omega}_4$) decreases as α increases (b) also for Pinned-Pinned vibrating configuration and a fixed value of α , an increase in value of n leads to a decrease in the values of frequencies ($\bar{\omega}_1, \bar{\omega}_2$) while a reverse trend holds for frequencies ($\bar{\omega}_3, \bar{\omega}_4$) (c) On the other hand, for both Clamped-Clamped and Clamped-Pinned vibrating configurations, it is seen that (i) for a fixed value of α , an increase in the values of n results in a decrease in the value of the first frequency ($\bar{\omega}_1$) of the system under consideration, whereas a reverse trend holds for the frequencies ($\bar{\omega}_2, \bar{\omega}_3, \bar{\omega}_4$). In other words, each of these non-fundamental frequencies increases (ii) for the same vibrating configurations in result c(i) stated above but for a fixed value of n , a rise in the value of α leads to a drop in the natural frequencies regardless of whether they are fundamental or not.

Table 6: Effect of non-homogeneity parameter (n) and non-uniformity parameter (α) on eigenfrequencies of a Simply Supported AFG pipe transporting flowing fluid supported by a Shear layer foundation ($\xi = 0.3, \beta = 0.5, \bar{v} = 2, G_p = 2.5, \bar{K}_w = 100, \gamma = 5, r = 0.02$)

α	n	$\bar{\omega}_1$	$\bar{\omega}_2$	$\bar{\omega}_3$	$\bar{\omega}_4$
0	1	13.3153	26.3902	43.1778	53.7160
	2	12.7738	26.3347	43.5317	54.9656
	3	12.5518	26.3055	43.6954	55.5623
0.1	1	13.4140	26.1606	42.8510	52.7793
	2	12.8412	26.0781	43.1952	53.8628
	3	12.6086	26.0297	43.3524	54.3330
0.3	1	13.6839	25.6861	42.0225	51.4380
	2	13.0404	25.5186	42.3107	52.1688
	3	12.7763	25.4129	42.4311	53.4832
0.5	1	14.0864	25.2913	40.9616	50.2300
	2	13.3665	24.9742	41.1307	51.8362
	3	13.0684	24.7712	41.1730	52.0909

Table 7: Effect of non-homogeneity parameter (n) and non-uniformity parameter (α) on eigenfrequencies of Clamped-Clamped AFG pipes transporting flowing fluid supported by a Shear layer foundation ($\xi = 0.2, \beta = 0.1, \bar{\nu} = 1, G_p = 1, \bar{K}_w = 100$)

α	n	$\bar{\omega}_1$	$\bar{\omega}_2$	$\bar{\omega}_3$	$\bar{\omega}_4$
0	1	16.0692	27.7717	42.6113	58.3224
	2	15.8069	28.0085	43.6250	60.0976
	3	15.7294	28.2007	44.2233	61.0826
0.1	1	15.9910	27.4519	42.0309	57.5894
	2	15.7230	27.6954	43.0395	59.3685
	3	15.6365	27.8855	43.6357	60.3614
0.3	1	15.8064	26.6491	40.5979	55.7217
	2	15.5235	26.9005	41.5904	57.4900
	3	15.4157	27.0829	42.1811	58.4920
0.5	1	15.5948	25.5526	38.6570	53.1252
	2	15.2913	25.7983	39.6179	54.8562
	3	15.1570	25.9643	40.1950	55.8561

Table 8: Effect of non-homogeneity parameter (n) and non-uniformity parameter (α) on eigenfrequencies of Clamped-Pinned AFG pipes with flowing fluid supported by a Shear layer foundation ($\xi = 0.2, \beta = 0.1, \bar{\nu} = 1, G_p = 1, \bar{K}_w = 100$)

α	n	$\bar{\omega}_1$	$\bar{\omega}_2$	$\bar{\omega}_3$	$\bar{\omega}_4$
0	1	14.8246	27.0903	42.3186	58.2952
	2	14.5730	27.4219	43.4181	60.0766
	3	14.4375	27.6302	44.0464	61.0484
0.1	1	14.8200	26.6806	41.6521	57.5138
	2	14.5593	27.0112	42.7451	59.3380
	3	14.4198	27.2142	43.3698	60.3437
0.3	1	14.8184	25.7151	40.0132	55.4658
	2	14.5350	26.0317	41.0781	57.2960
	3	14.3833	26.2188	41.6890	58.3189
0.5	1	14.8117	24.5258	37.8386	52.6126
	2	14.5194	24.8062	38.8458	54.3922
	3	14.3691	24.9657	39.4280	55.4024

Effect of Pasternak foundation parameters on vibration of an AFG Timoshenko tapered pipes

The impact of Pasternak foundation stiffnesses on the vibration characteristics of an AFG fluid-carrying Timoshenko piping systems subjected to each of Clamped-Clamped, Pinned-Pinned and Clamped-Pinned end conditions is shown in Tables 9-11. The computations for this numerical example involved the following data: $\alpha = 0.2, \beta = 0.5, \xi = 0.3, \bar{\nu} = 2, n = 2$ with various values of the foundation stiffness. It is hereby remarked that foundation stiffnesses whose values are zero represent the case when the pipe is not resting on foundation. It is observed from Tables 9-11 that the eigenfrequency increases with an increase in the Winkler parameter \bar{K}_w for a fixed value of G_p . Similarly, the eigenfrequencies increases with an increase in shear layer of the foundation stiffness parameter G_p . Hence, the influence of foundation stiffnesses play a prominent role on the dynamic response of the AFG thick pipes with flowing fluid supported by a variable Shear layer foundation.

Table 9: Effect of spring constant and shear layer stiffness parameters on the vibration of AFG tapered Timoshenko pipes with flowing fluid subjected to Pinned-Pinned support

\bar{K}_w	G_p	$\bar{\omega}_1$	$\bar{\omega}_2$	$\bar{\omega}_3$	$\bar{\omega}_4$
0	0	4.4643	18.9296	34.4924	50.1340
	1	5.3337	19.8658	37.4098	51.5724
10	2.5	6.4331	21.1923	37.4098	53.7514
	10	10.3812	26.8643	45.0031	63.1085
	0	5.3246	19.1670	34.6221	50.2240
	1	6.0774	20.0920	35.8153	51.6591
100	2.5	7.0679	21.4045	37.5298	53.8351
	10	10.7976	27.0322	45.1035	63.1822
	0	10.2055	21.1833	35.7689	51.0267
	1	10.6445	22.0230	36.9262	52.4332
1000	2.5	11.2716	23.2261	38.5927	54.5826
	10	13.9976	28.4987	45.9965	63.8455
	0	29.3652	35.4837	45.6674	58.4976
	1	29.6054	35.9951	46.5898	59.6164
	2.5	29.9461	36.7480	47.9303	61.5617
	10	31.4177	40.3127	54.1091	70.1904

Table 10: Effect of spring constant and shear layer stiffness parameters on the vibration of AFG tapered Timoshenko pipes with flowing fluid subjected to Clamped-Clamped support

\bar{K}_w	G_p	$\bar{\omega}_1$	$\bar{\omega}_2$	$\bar{\omega}_3$	$\bar{\omega}_4$
0	0	9.5474	22.0023	36.0185	50.8953
	1	10.0464	22.8217	37.1659	52.2892
	2.5	10.7500	23.9989	38.8202	54.4371
10	10	13.7161	29.1879	46.1755	63.5712
	0	9.9784	22.2100	36.1431	50.9841
	1	10.4605	23.0218	37.2867	52.3746
	2.5	11.1422	24.1890	38.9360	54.5197
100	10	14.0362	29.3443	46.2733	63.6455
	0	13.2409	23.9980	37.2455	51.7768
	1	13.6322	24.7497	38.3570	53.1369
	2.5	14.1919	25.8375	39.9632	55.2577
1000	10	16.6419	30.7166	47.1442	64.3155
	0	30.5526	37.4125	46.8540	59.1861
	1	30.8194	37.8994	47.7457	60.2120
	2.5	31.1952	36.6183	49.0511	62.1629
	10	32.7803	42.0414	55.0820	70.6918

Table 11: Effect of spring constant and shear layer stiffness parameters on the vibration of AFG tapered Timoshenko pipes with flowing fluid subjected to Clamped-Pinned support

\bar{K}_w	G_p	$\bar{\omega}_1$	$\bar{\omega}_2$	$\bar{\omega}_3$	$\bar{\omega}_4$
0	0	7.9547	21.0884	35.6156	50.7131
	1	8.5590	21.9497	36.7776	52.1366
	2.5	9.3882	23.1804	38.4514	54.2659
10	10	12.7048	28.5408	45.8777	63.5290
	0	8.4691	21.3038	35.7417	50.8022
	1	9.0429	22.1567	36.9003	52.2098
	2.5	9.8358	23.3763	38.5685	54.3583
100	10	13.0496	28.7004	45.9768	63.7722
	0	12.1565	23.1519	36.8574	51.5972
	1	12.5870	23.9383	37.9830	52.9761
	2.5	13.1976	25.0710	39.6066	55.0988
1000	10	15.8175	30.0984	46.8543	64.2694
	0	30.1423	36.8161	46.5569	59.0097
	1	30.4076	37.3205	47.4612	60.0962
	2.5	30.7815	38.0613	48.7756	62.0195
	10	32.3642	41.5642	54.8510	70.5495

Effects of mass ratio β and flow velocity \bar{v} on the eigenfrequencies of AFG Timoshenko pipes with flowing fluid supported by a variable Pasternak elastic subgrade

This section investigates how the first four dimensionless eigenfrequencies of an inhomogeneous materials, non-uniform Timoshenko pipe transporting internal fluid and supported by a bi-parametric elastic subgrade vary with changes in mass ratio and flow velocity. The results, summarized in Tables 12–14, illustrate the dependence of the frequencies on these parameters. The study considers three boundary conditions: Pinned–Pinned, Clamped–Pinned, and Clamped–Clamped. The parameters used in the analysis are $\xi = 0.3$, $\alpha = 0.2$, $n = 2$, $\bar{K}_w = 10$, $G_p = 2.5$.

The findings reveal that, for a fixed mass ratio β , increasing the fluid velocity \bar{v} leads to a decrease in the natural frequencies of the pipe. Similarly, when the fluid velocity is fixed, an increase in the mass ratio β results in lower eigenfrequencies across all boundary conditions. These results highlight the destabilizing effects of both flow velocity and the mass ratio on the system's dynamic behavior.

Table 12: Impact of mass ratio (β) and flow velocity (\bar{v}) on the eigenfrequencies of AFG non-uniform Pinned-Pinned Timoshenko pipes with flowing fluid lying on Pasternak subgrade

β	\bar{v}	$\bar{\omega}_1$	$\bar{\omega}_2$	$\bar{\omega}_3$	$\bar{\omega}_4$
0.1	0	9.3749	25.1885	43.3975	62.0021
	1	8.9818	24.6379	42.6566	61.0630
	2	7.7013	22.9167	40.3577	58.1383
0.3	0	9.1441	24.5009	42.1878	60.2473
	1	8.7223	23.9210	41.3726	59.1700
	2	7.3649	22.1227	38.8622	55.8599
0.5	0	8.9273	23.8747	41.0778	58.5806
	1	8.4821	23.2697	40.2032	57.4080
	2	7.0679	21.4045	37.5298	53.8351

Table 13: Impact of mass ratio (β) and flow velocity (\bar{v}) on the eigenfrequencies of AFG non-uniform Clamped-Pinned Timoshenko pipes with flowing fluid lying on Pasternak subgrade

β	\bar{v}	$\bar{\omega}_1$	$\bar{\omega}_2$	$\bar{\omega}_3$	$\bar{\omega}_4$
0.1	0	13.5457	27.9032	44.7674	62.0276
	1	13.2451	27.4022	44.0463	61.1755
	2	12.3055	25.8491	41.8147	58.4676
0.3	0	13.1404	27.1376	43.5523	60.6405
	1	12.7858	26.6132	42.7492	54.6239
	2	11.6809	24.9973	40.2896	56.4525
0.5	0	12.7653	26.4274	42.4232	59.1292
	1	12.3677	25.8785	41.5592	57.9974
	2	11.1422	24.1890	38.9360	54.5197

Table 14: Impact of mass ratio (β) and flow velocity (\bar{v}) on the eigenfrequencies of AFG non-uniform Clamped-Clamped Timoshenko pipes with flowing fluid lying on Pasternak subgrade

β	\bar{v}	$\bar{\omega}_1$	$\bar{\omega}_2$	$\bar{\omega}_3$	$\bar{\omega}_4$
0.1	0	12.1777	27.0888	44.3536	62.0276
	1	11.8640	26.5740	43.6254	61.1639
	2	10.8813	24.9758	41.3707	58.4040
0.3	0	11.7959	26.3659	43.1679	60.5760
	1	11.4372	25.8239	42.3629	59.5369
	2	10.3194	24.1519	39.8921	56.3114
0.5	0	11.4447	25.6962	42.0667	59.0235
	1	11.0508	25.1268	41.2019	57.8745
	2	9.8358	23.3763	38.5685	54.3583

Effect of rotatory inertia parameter (r) and the foundation modulus variability parameter (ξ) on the eigenfrequencies of AFG non-prismatic Timoshenko pipeline with variable cross-section supported

The effect of the rotatory inertia parameter (r) on the eigenfrequencies of AFG Timoshenko pipes with variable cross-section supported by Pasternak elastic subgrade is evaluated to deepen the understanding of its vibrational behaviour. Figures 1 to 3 present the frequency variation for different values of the foundation's non-uniformity parameter (ξ) under Pinned-Pinned, Clamped-Pinned, and Clamped-Clamped end conditions. The adopted system parameters include: $\bar{v} = 2$, $n = 1$, $G_p = 2.5$, $\bar{K}_w = 10$, $\alpha = 0.3$, $\beta = 0.5$. The numerical results reveal a clear decreasing trend in natural frequencies with increasing r , even as ξ is kept constant. Furthermore, an increase in ξ results in frequency reduction, regardless of the boundary condition. These findings emphasize the critical role of rotatory inertia and foundation stiffness variability in the dynamic analysis of AFG piping system.

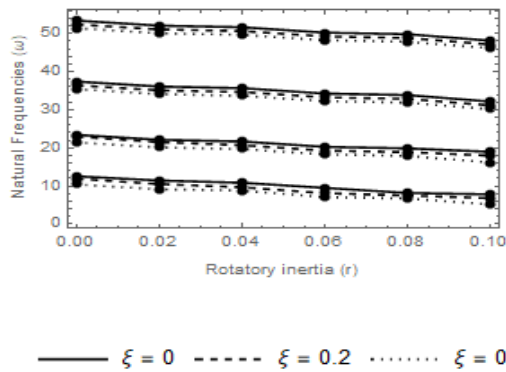


Fig. 1: Impacts of r and ξ on the eigenfrequencies of an AFG Pinned-Pinned Timoshenko pipe with fluid flowing supported by a foundation

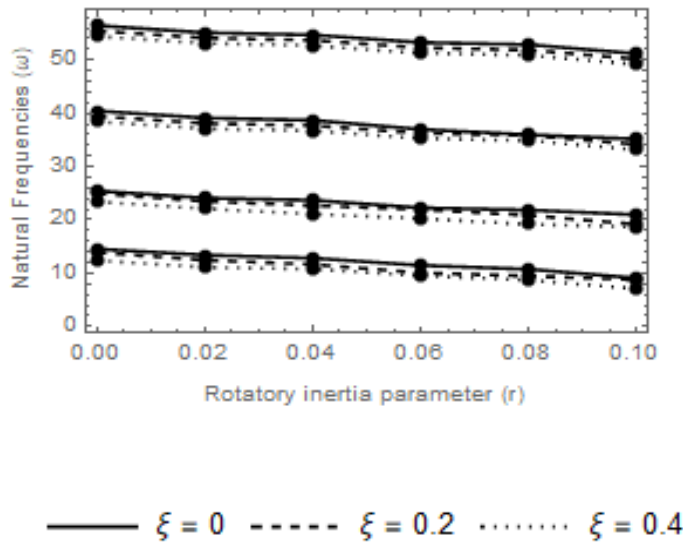


Fig. 2: Impacts of r and ξ on the eigenfrequencies of an AFG Clamped-Pinned Timoshenko pipe with fluid flowing supported by a foundation

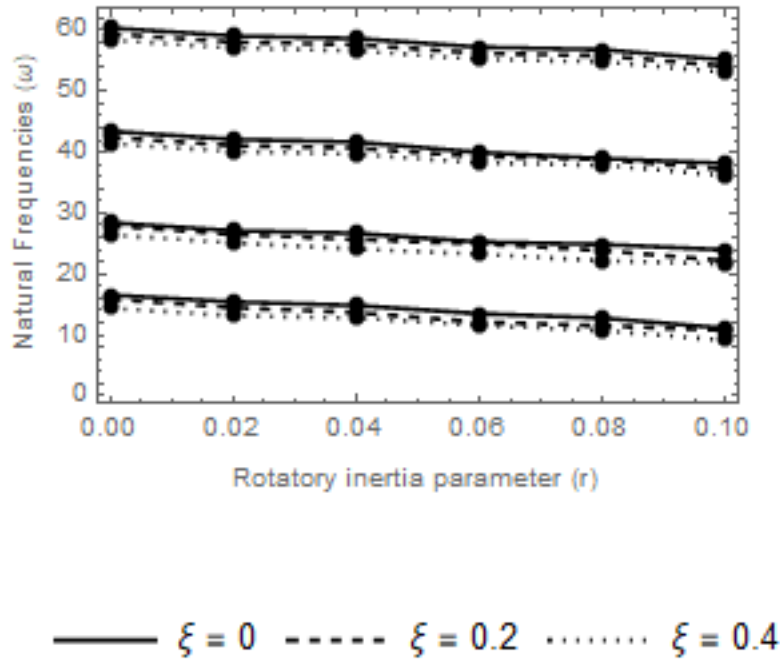


Fig. 3: Impacts of r and ξ on the eigenfrequencies of an AFG Clamped-Clamped Timoshenko pipe with fluid flowing supported by a foundation

Vibration of an AFG Timoshenko pipe with flowing fluid under different values of tapering parameter α

Figures 4-6 illustrate the variation of the eigenfrequencies of an inhomogeneous non-prismatic Timoshenko pipe with flowing fluid supported by Pasternak subgrade for various values of α . Also, $\xi = 0.3$, $\beta = 0.1$, $\bar{\nu} = 1$, $n = 2G_p = 1$, $\bar{K}_w = 100$. For the Timoshenko pipe subjected to Clamped-Clamped, Clamped-Pinned, and Pinned-Pinned end conditions, the effect of the tapering parameter α on eigenfrequencies of the piping system was investigated. In the Clamped-Clamped and Clamped-Pinned cases, all natural frequencies exhibit a decreasing trend as α increases. In contrast, the Pinned-Pinned case reveals a distinct behavior where $(\bar{\omega}_1, \bar{\omega}_2)$ increase with α , while $(\bar{\omega}_3, \bar{\omega}_4)$ decrease with increasing α .

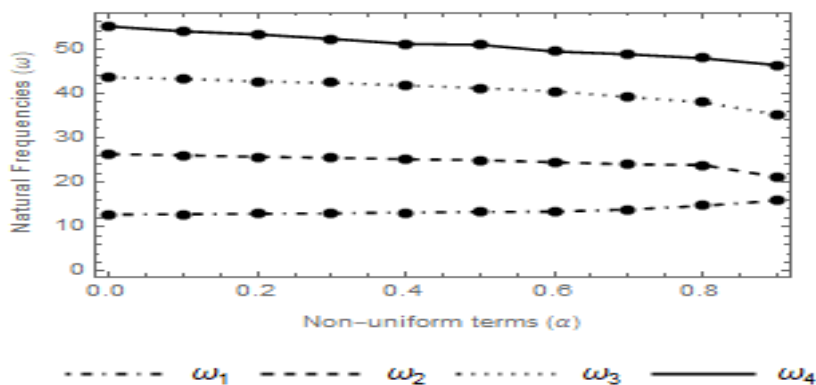


Fig.4: Influence of the tapering parameter α of the pipe on the eigenfrequencies of AFG tapered Pinned-Pinned Timoshenko piping system

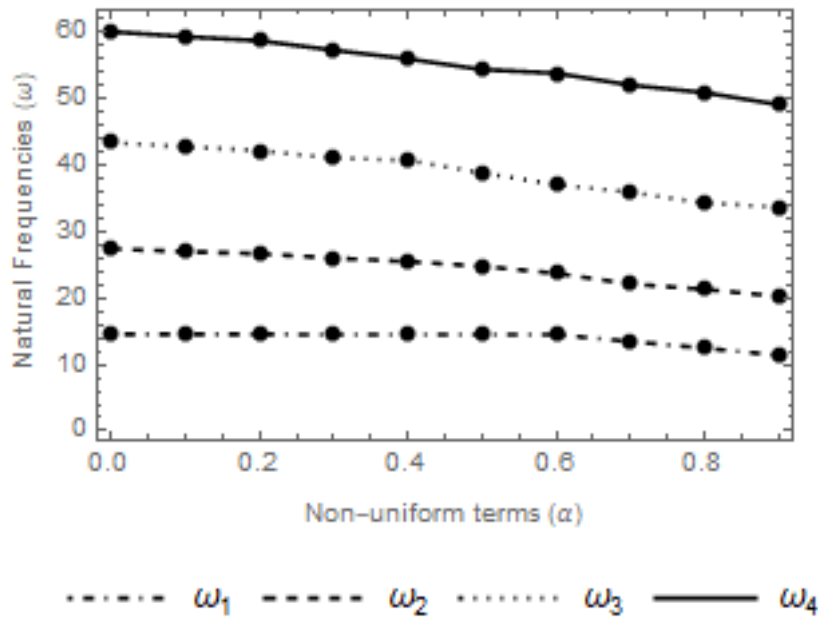


Fig. 5: Influence of the tapering parameter α of the pipe on the eigenfrequencies of AFG tapered Clamped-Pinned Timoshenko piping system

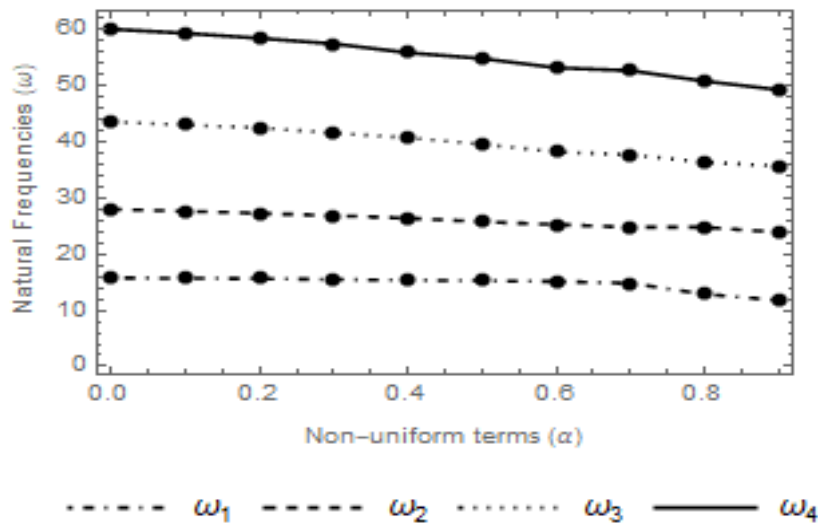


Fig. 6: Influence of the tapering parameter α of the pipe on the eigenfrequencies of AFG tapered Clamped-Clamped Timoshenko piping system

Convergence studies

It is first remarked at this juncture that in all the numerical computations carried out in the above section, convergence issue is dependent on the number of iterations (m) such that

$$|\omega_i^{(m)} - \omega_i^{(m-1)}| \leq \epsilon$$

In the above inequality, ϵ denotes the tolerance parameter whose value is 1×10^{-5} [Bozygit et al (2017)]. However, in cases where the convergence criterion described in the above expression is not satisfied, the computational procedure is repeated by increasing the number of iterations (m) until convergence is attained.

Figures 7-9 illustrate the convergence of the first four dimensionless eigenfrequencies of an internally flowing AFG non-prismatic Timoshenko pipe supported by a variable Pasternak subgrade using VIM. The data used for this computation are $\alpha = 0.2$, $\beta = 0.5$, $n = 1$, $\bar{v} = 2$, $\xi = 0.3$, $G_p = 2.5$, and $\bar{K}_w = 10$ for each of the three vibrating configuration: Pinned-Pinned, Clamped-Pinned and Clamped-Clamped end conditions. It is seen that the natural frequencies are plotted against the number of iteration. The natural frequencies obtained using the present procedure (VIM) converge rapidly to the approximate solutions as the iteration step increases. This implies that, higher eigenfrequencies are obtained with high number of iteration.

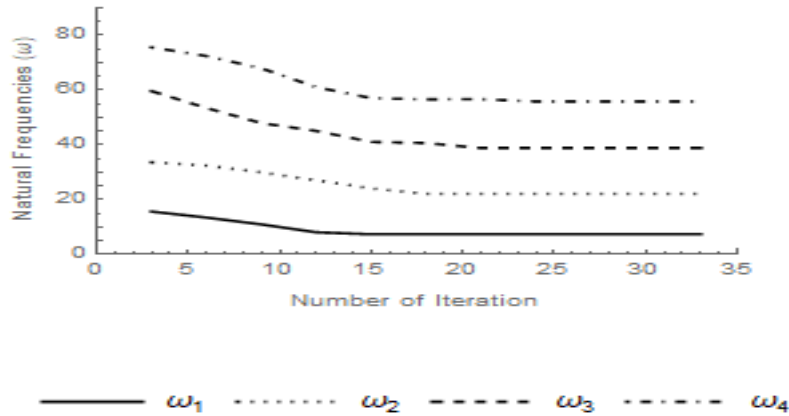


Fig. 7: Influence of rotary inertia coefficient r and the tapering foundation parameter ξ on the eigenfrequencies of an AFG Pinned-Pinned Timoshenko pipes lying on a bi-parametric elastic subgrade

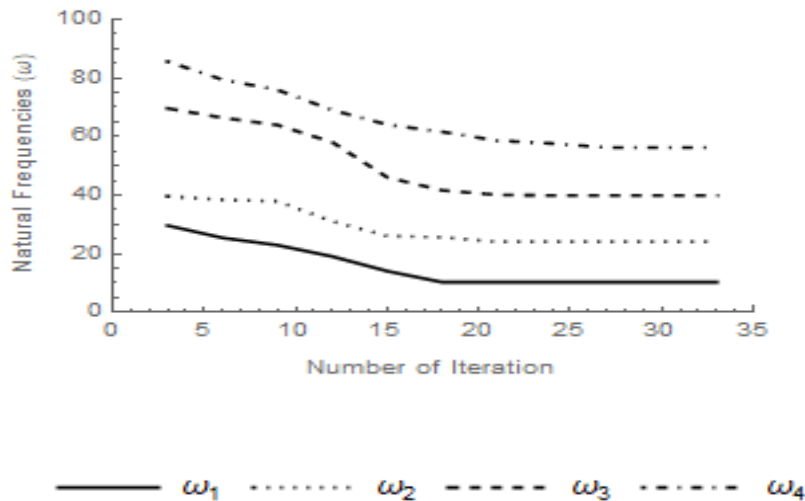


Fig. 8: Influence of rotary inertia coefficient r and the tapering foundation parameter ξ on the eigenfrequencies of an AFG Clamped-Pinned Timoshenko pipes lying on a bi-parametric elastic subgrade

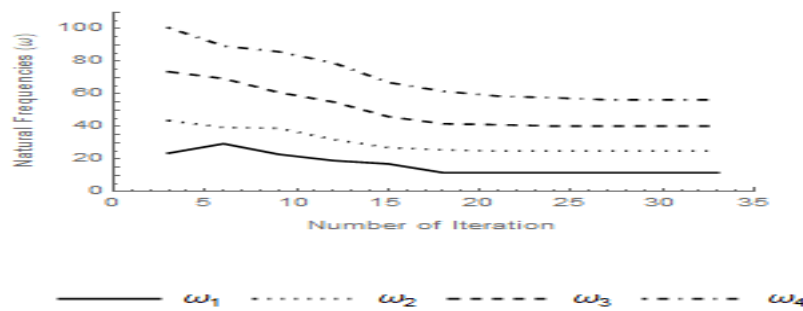


Fig. 9: Influence of rotary inertia coefficient r and the tapering foundation parameter ξ on the eigenfrequencies of an AFG Clamped-Clamped Timoshenko pipes lying on a bi-parametric elastic subgrade

Conclusion

In this study, the flow-induced vibration of an AFG, non-uniform Timoshenko pipe conveying internal fluid and lying on Pasternak elastic subgrade is investigated using a semi-analytical technique, namely the **Variational Iteration Method (VIM)**. Three end-support configurations are considered: Pinned–Pinned, Clamped–Pinned, and Clamped–Clamped. The natural frequencies of the system are evaluated and compared with results available in the literature to verify the accuracy and reliability of the proposed approach. Based on the numerical results obtained, the following conclusions are drawn:

- i. The numerical results obtained in the present work are validated by comparing the VIM solutions with the results gotten from the available published articles for the cases considered under the three vibrating configuration, and a good agreement is observed.
- ii. Results are obtained for the impact of both the non-uniform parameter α , and material gradient index n on the eigenfrequencies of an AFG non-uniform Timoshenko pipe with flowing fluid lying on a variable Pasternak subgrade subjected to the three different boundary conditions. It can be observed that for Pinned-Pinned vibrating configuration, and for a fixed value of n , the fundamental frequency increases, while each of the non-fundamental frequencies decreases as α increases. Also, for the same vibrating configuration and a fixed value of α , an increase in value of n leads to a decrease in the value of frequencies $(\bar{\omega}_1, \bar{\omega}_2)$ while a reverse trend holds for frequencies $(\bar{\omega}_3, \bar{\omega}_4)$. On the other hand, for Clamped-Clamped and Clamped-Pinned vibrating configurations, it is seen that for a fixed value of α , an increase in the values of n results in the value of the fundamental frequency $(\bar{\omega}_1)$ of the system under consideration, whereas a reverse trend holds for the frequencies $(\bar{\omega}_2, \bar{\omega}_3, \bar{\omega}_4)$. Also, for the same vibrating configuration, and for a fixed value of n , an increase in the value of α leads to a decrease in the eigenfrequencies regardless of whether they are fundamental or not.
- iii. The impact of the mass ratio β , and velocity \bar{v} on the frequencies of the system under consideration for each of the three vibrating configurations are examined. It is seen that as the fluid velocity increases with β being fixed, the eigenfrequencies of the pipe decrease. Also, a depreciation is observed in the values of the eigenfrequency for a fixed value of \bar{v} as β increases for all the three sets of the end conditions.
- iv. The effect of Shear layer stiffness and Winkler spring stiffness on the eigenfrequencies of the AFG non-prismatic Timoshenko pipes carrying flowing fluid under each of the three vibrating configurations is investigated. It is observed that the eigenfrequencies increase with an increase in the stiffness of Winkler parameter \bar{k}_w . Also, the eigenfrequencies increase with an increase in shear layer of the foundation stiffness parameter G_p . Hence, the influence of foundation stiffnesses play a prominent role in the dynamic behaviour of an AFG Timoshenko pipes with variable cross-section lying on a bi-parametric subgrade.
- v. The influence of the rotary inertia coefficient (r) and the tapering foundation parameter (ξ) on the eigenfrequencies of the system under consideration is examined. It is observed that the values of the eigenfrequencies decrease with increasing rotary inertia coefficient r with the tapering foundation parameter ξ being held constant. Also, for the three vibrating configuration, the eigenfrequencies decrease with an increase in the tapering foundation parameter ξ . Hence, the presence of rotatory inertia parameter and the non-uniform parameter of the foundation affect the vibration analysis of an AFG fluid-carrying Timoshenko pipes resting on a bi-parametric subgrade.

Finally, the analysis carried out in the study revealed that a semi-analytical method (VIM) used is computationally efficient in solving the vibration problems involving AFG Timoshenko pipes with flowing fluid lying on a variable Pasternak subgrade. This is due to its high degree of accuracy and its fast convergence of the solution.

Declaration

The authors have no competing interest to declare that are relevant to the content of this article.

Funding

The authors did not receive support from any organization for the submitted work

Financial Interest

The authors declare they have no financial interest

Authors Contribution

Gbadeyan Jacob Abiodun was responsible for the study's conceptualization, mathematical analysis, methodology design, interpretation of results, and preparation of the original manuscript draft. Adeniran Paul Oluwafemi contributed to the mathematical analysis, developed and implemented the computational codes, carried out the numerical analysis, participated in the discussion of results, and assisted in drafting the original manuscript.

References

- Adair D., Ismailov K., & Jaeger M (2018). Vibration of beam on an elastic foundation using the variational iteration method. *International Journal of Aerospace and Mechanical Engineering*, 12(9), 914-919
- Aghazadeh R., (2021) Dynamics of axially functionally graded pipes conveying fluid using a Higher Order Deformation Theory. *International Advanced Researches and Engineering Journal*, 209 – 217
- Auciello., N.M., & Ercolano, A. (2004). A general solution for dynamic response of axially loaded non-uniform Timoshenko beams. *International Journal of Solids and Structures*, 41, 4861-4874
- Askarian, A.R., Permoon, M.R., Rahmanian, M. (2024). Stability analysis of fluid conveying Timoshenko pipes resting on fractional viscoelastic foundations. *Mechanics Research Communications*, 144, 1-22
- Bozyigit, B., Yesilce Y., & Catal, S. (2017). Differential Transform Method and Adomian Decomposition Method to free vibration analysis of fluid conveying pipelines. *Structural Engineering and Mechanics*, 62(1), 65-77
- Calim, F.F. (2016) Transient analysis of axially functionally graded Timoshenko beams with variable cross-section. *Composites Part B: Engineering*, 98, 472-483
- Chellapilla, K.R., & Simha HS (2007). Critical velocity of fluid conveying pipe resting on two-parameter foundation. *Journal of Sound and Vibration*, 302, 387-397
- Chen, Y., Dong, S., Zang, Z., Gao, M., Zhang, J., Ao C., Liu, H., & Zhang, Q. (2020). Free transverse vibration analysis of functionally graded tapered beams via the Variational Iteration Method. *Journal of Vibration and Control*, 1(15), 1-16
- Chu, C.L., & Lin, L.H. (1995). Finite Element Analysis of fluid-conveying Timoshenko pipes. *Shock and Vibration* 58, 247-255
- Dagli, B.Y., Ergut, A. (2019). Dynamics of fluid-conveying pipes using Rayleigh theory under classical boundary conditions. *European Journal of Mechanics/ B. Fluids*, 1-22
- Dangal, M., & Ghimire, S.K. (2019). Modeling and analysis of flow induced vibration in pipes using Finite Element Approach. *Proceedings of IOE Graduate Conference*, 6(5), 725-732
- Ding, H., Chen, L.Q., & Tang, X.T. (2019). Nonlinear frequencies and forced responses of pipe conveying fluid via a coupled Timoshenko model. *Journal of Sound and Vibration*, 1-23
- Ding, H., & Ji, J.C. (2023) Vibration control of fluid-conveying pipes: A state of the art reviewed. *Applied Mathematics and Mechanics*, 44(9), 1423-1456
- Ding, Y.H., Chen, Z.Q., & Liang, F. (2024). Flexural vibration control of functionally graded poroelastic pipes via periodic piezoelectric design. *Acta Mech*, 235, 3131–3147 <https://doi.org/10.1007/s00707-024-03879-1>
- Elthaher, M.A., Alshorbagy, A.E., & Mahmoud, F.F. (2010) Free vibration characteristics of a functionally graded beam by Finite Element Method. *Applied Mathematical Modelling*, 2(35), 412-425
- Fang, J., & Zhou, D. (2017). Three-dimensional vibration of rotating functionally graded beams. *Journal of Vibration and Control*, 24(15), 1-15
- Gaith, M. (2021). The vibration of simply supported non-uniform cross-sectional pipe conveying fluid resting on a viscoelastic foundation. *WSEAS Transactions on Fluid Mechanics*, 2(15): 163-171
- Gbadeyan, J.A., & Adeniran, P.O. (2023). Flow-induced vibration and stability analyses of axially functionally graded non-prismatic fluid-conveying pipes resting on variable non-Winkler foundation. *International Journal of Engineering Research and Applications*, 3(13), 149 – 176

- Huang Y, Yang, L.E, & Luo, Q.Z (2013). Free vibration of axially functionally graded Timoshenko beams with non-uniform cross-section. *Composites: Part B*, **45**, 1493-1498
- Jiya, M., Inuwa, Y.I., & Shaba, A.I. (2018). Dynamic response analysis of uniform conveying fluid pipe on two parameter elastic foundation. *Science World Journal*, 2(13), 1-5
- Li, Z.H., & Liu, T. (2022). Non-Linear vibration analysis of functionally graded material tubes with conveying fluid resting on elastic foundation by a new tubular beam model. *International Journal of Non-Linear Mechanics*, 137, 1 – 13
- Misra, A.K., Padoussis, M.P., & Van, K.S. (1999). On the dynamics of curved pipes transporting fluid: Extensible theory. *Journal of Fluids and Structures*, 2(3), 245-261
- Miyamoto, Y., Kaysser, W.A., & Rabbin, B.H. (1999). *Functionally Graded Materials: Design Processing and Applications* Boston. *Kluwer Academic Publishers*
- Ozdemir, O. (2019). Vibration analysis of rotating Timoshenko beams with different material distribution properties. *Selcuk Univ. J. Eng. Sci. Tech*, 7(2), 272-286
- Paidoussis, M.P., Kheiri, M., Del-Pozo, G.C., & Amabali, M. (2014). Dynamics of a pipe conveying fluid flexibly restrained at the ends. *Journal of FLuids and Structures*, 49, 360-385
- Sakar, K., & Ganguli, R. (2014). Closed Form Solution for Axially Functionally Graded Timoshenko Beams having Uniform Cross-section and Fixed-fixed Boundary Condition. *Composites Part B*, 58, 361-370
- Shahba, A., Attarnejad, R., & Semnani S.J. (2010). Application of Differential Transformation Method in free vibration analysis of Timoshenko beams resting on two-parameter elastic foundation. *Arabian Journal for Science and Engineering*, 135, 125-132
- Soares, L.S., Bezerra, W.K., & Hoefel, S. (2017). Dynamic analysis of Timoshenko beams on Pasternak foundation. *Proceedings of the XXXVIII Iberian Latin-American Congress on Computational Methods in Engineering Brazil 41*: 1-14
- Soltani, M., & Asgarian, B. (2019). New Hybrid Approach for free vibration and stability analyses of axially functionally graded Euler-Bernoulli beams with variable cross-section resting on uniform Winkler-Pasternak foundation. *Latin American Journal of Solids and Structures*, 16(3), 1-25
- Sutar, S., Madabhushi, R., Chellapilla, K.R., & Poosa, R.B. (2018). Determination of natural frequencies of fluid-conveying pipes using Muller's Method. *J. Insti. Eng. India Ser.*, 1-6
- Talib, E.E., Emman, R.B., & Sadiq, M.H. (2019). Differential Quadrature Method for dynamic behaviour of functionally graded materials pipe conveying fluid on visco-elastic foundation. *University of Thi-Qar Journal for Engineering Sciences*, 1(110), 50-64
- Tang, A.Y., Wu, J.X., Li, X.F., & Lee, K.Y. (2014). Exact frequency equations of free vibration of exponentially non-uniform functionally graded Timoshenko beams. *International Journal of Mechanical Sciences*, 1-30
- Tang Y., Bian, P., & Qing, H. (2025). Buckling and free vibration analyses of functionally graded timoshenko nanobeams resting on elastic foundation. *Int. J. Dynam. Control*, 13(113), <https://doi.org/10.1007/s40435-025-01614-9>
- Yi-min, H., Young-Shoul, L., Bao-hui, L., Yan-jiang, L., & Zhu-feng, Y. (2010). Natural Frequency Analysis of Fluid Conveying Pipeline with Different Boundary Conditions. *Nuclear Engineering and Design*, 240, 461-467
- Yang, X.D., Liang, F., Bao, R.D., Zhang, W. (2016). Frequency analysis of functionally graded curved pipes conveying fluid. *Advances in Materials Science and Engineering*, 1 – 9
- Yi-wen, Z., & Gui-Lin, S. (2022) Wave propagation and vibration of functionally graded pipes conveying hot fluid. *Steel and Composite Structures*, 42(3), 397 – 405
- Zhao, Y., Huang, Y., & Guo, M. (2017). A novel approach of free vibration of axially functionally graded beams with non-uniform cross-section based on Chebyshev Polynomials Theory. *Composite Structures*, 1-26
- Zhao, Y., Hu, D., Wu, S., Long, X., & Liu, Y. (2021). Dynamics of axially functionally graded conical pipes conveying fluid. *Journals of Mechanics* 37(1), 318-326